Journal of Alloys and Compounds xxx (2008) xxx–xxx

Contents lists available at ScienceDirect

Journal of Alloys and Compounds

journal homepage: www.elsevier.com/locate/jallcom

Influence of heavy rare earth ions substitution on microstructure and magnetism of nanocrystalline magnetite

Z. Cvejic[a], B. Antic[b,*], A. Kremenovic[b,c], S. Rakic[a], G.F. Goya[d], H.R. Rechenberg[d], C. Jovalekic[e], V. Spasojevic[b]

[a] Institute of Physics, Faculty of Natural Sciences, University of Novi Sad, Trg D. Obradovica 6, 21000 Novi Sad, Serbia
[b] Institute of Nuclear Sciences "Vinca", Solid State Physics Laboratory, P.O. Box 522, 11001 Belgrade, Serbia
[c] Faculty of Mining and Geology, Laboratory for Crystallography, University of Belgrade, Djusina 7, 11000 Belgrade, Serbia
[d] Instituto de Fisica, Universidade de Sao Paulo, CP 66318, 05315-970 Sao Paulo SP, Brazil
[e] Center for Multidisciplinary Studies, University of Belgrade, Kneza Viseslava 1, 11000 Belgrade, Serbia

ARTICLE INFO

Article history:
Received 26 March 2008
Received in revised form 2 May 2008
Accepted 11 May 2008
Available online xxx

Keywords:
Oxide materials
Mechanochemical processing
Microstructure
Magnetic measurements
X-ray diffraction

ABSTRACT

In this work we report results on the influence of heavy rare earth ions substitution on microstructure and magnetism of nanocrystalline magnetite. A series of $Fe_{2.85}RE_{0.15}O_4$ (RE = Gd, Dy, Ho, Tm and Yb) samples have been prepared by high energy ball milling. Structure/microstructure investigations of two selected samples $Fe_{2.85}Gd_{0.15}O_4$ and $Fe_{2.85}Tm_{0.15}O_4$, represent an extension of the previously published results on Fe_3O_4/γ-Fe_2O_3, $Fe_{2.85}Y_{0.15}O_4$ and $Fe_{2.55}In_{0.45}O_4$ [Z. Cvejic, S. Rakic, A. Kremenovic, B. Antic, C. Jovalekic, Ph. Colomban, Sol. State Sciences 8 (2006) 908], while magnetic characterization has been done for all the samples.Crystallite/particle size and strain determined by X-ray diffractometry and Transmission electron microscopy (TEM) confirmed the nanostructured nature of the mechanosynthesized materials. X-ray powder diffraction was used to analyze anisotropic line broadening effects through the Rietveld method. The size anisotropy was found to be small while strain anisotropy was large, indicating nonuniform distribution of deffects in the presence of Gd and Tm in the crystal structure. Superparamagnetic (SPM) behavior at room temperature was observed for all samples studied. The Y-substituted Fe_3O_4 had the largest H_C and the lowest M_S. We discuss the changes in magnetic properties in relation to their magnetic anisotropy and microstructure. High field irreversibility ($H > 20$ kOe) in ZFC/FC magnetization versus temperature indicates the existence of high magnetocrystalline and/or strain induced anisotropy.

1. Introduction

Magnetite (Fe_3O_4) has been the focus of intense research since centuries ago due to its unique magnetic properties. Currently, this interest is still active because novel magnetic properties have been reported in nanostructured magnetite systems, such as films and nanoparticles. From the industrial point of view, magnetite is a key material for magnetic seals, recording media, sensors, catalysts, etc. [2,3]. In biomedical application magnetite was the most frequently used as core in magnetic functionalized particles that were used in magnetic fluid hyperthermia, as contrast agent for magnetic resonance imaging, in magnetic assisted chemical separation, as magnetic drug carriers [4,5].

Magnetite crystallizes in spinel structure type with space group (SG) $Fd\bar{3}m$. Iron ions occupy both tetrahedral A (8a) $\bar{4}3m$ and octahedral B (16d) $\bar{3}m$ sites, while oxygen are in the 32e 3m position. It is an inverse spinel with metal conductivity at room temperature [6]. From magnetic point of view, magnetite is a ferrimagnet, with strong exchange interaction between A and B sites ($J_{A-B} > J_{A-A}, J_{B-B}$).

Partial cation substitution of iron in magnetite offers a possibility to improve and control its physical and chemical properties. Cation substitution in spinels may be at one or both cation sites, with magnetic or non-magnetic ions with different valence. It is possible to change crystal symmetry by substitution and form cation deficit spinels with changing cation valence [7]. Cations incorporated in spinel lattice change magnetic interactions and magnetic anisotropy, influencing the saturation magnetization and coercivity values of parent compounds. Rare earth substituted spinels have been earlier investigated [8,9]. It was shown that Curie temperature decreases and coercivity field increase with rare earth substitution in Ni, Zn ferrites [8]. In Ho-substituted Fe_3O_4

* Corresponding author. Tel.: +381 11 8065829; fax: +381 11 8065829.
E-mail address: bantic@vin.bg.ac.yu (B. Antic).

0925-8388/$ – see front matter © 2008 Elsevier B.V. All rights reserved.
doi:10.1016/j.jallcom.2008.05.026

the energy barrier height is drastically modified and the blocking temperature shifts towards lower temperatures [9]. For some specific clinical and industrial applications magnetite is required to have improved magnetic performance such as high saturation magnetization and coercivity. Also, small size particles with narrow particle size distribution are sometimes required for bio-applications, which must be non-toxic and biocompatible [10]. Systematic studies in rare earth substituted magnetite may give correlation between type of rare earth ion and magnetic parameters, and select candidates for a particular application.

In a previous paper [1] we reported results on structural, microstructural and Raman investigation on Fe_3O_4/γ-Fe_2O_3, $Fe_{2.85}Y_{0.15}O_4$ and $Fe_{2.55}In_{0.45}O_4$. In the present work, we aim: (i) synthesize heavy rare earth (Gd, Dy, Ho, Tm and Yb) substituted magnetite by high energy ball milling; (ii) analyze the resulting crystallite size/strain (taking into consideration previously published results [1]) in order to estimate the influence of the substitution on the microstructural parameters and (iii) determine the resulting magnetic properties and their correlation with structural and microstructural parameters.

2. Experimental

A mixture of crystalline powders of RE_2O_3 (RE = Gd, Dy, Ho, Tm and Yb) and Fe_2O_3 were used as starting material to produce $Fe_{2.85}RE_{0.15}O_4$ spinels. Mechanochemical treatment was performed in a planetary ball mill (Fritsch Pulferisette 5) for 20 h. A hardened-steel vial of 500 cm^3 volume, filled with hardened-steel balls of a diameter of 13.4 mm, was used as milling medium. The mass of the powder was 10 g and the balls-to-powder mass ratio was 20:1. The milling was done in air atmosphere without any additives. The angular velocity of the supporting disc and vial was 32.2 and 40.3 rad/s, respectively. The intensity of milling corresponded to an acceleration of about 10 times the gravitational acceleration. The samples Fe_3O_4/γ-Fe_2O_3, $Fe_{2.85}Y_{0.15}O_4$ and $Fe_{2.55}In_{0.45}O_4$ were previously prepared under the same conditions [1].

For the XRPD data collection a Philips PW1710 automated X-ray powder diffractometer was used. The diffractometer was equipped with a Cu-tube, graphite monochromator and Xe-filled proportional counter. The generator was set-up on 40 kV and 32 mA. Divergence and receiving slits were 1° and 0.1 mm, respectively. Data for the Rietveld refinement were collected in a step scan mode between 15° and 135° 2θ at every 0.03° 2θ. Transmission electron microscopy (TEM) measurement for sample $Fe_{2.85}Tm_{0.15}O_4$ was performed on Philips EM 400 equipment, with magnification up to 310000. Hysteresis loops were measured at 2 K after zero-field-cooling using an MPMS XL-5 SQUID magnetometer. The measurements were made in fields H from −50 to +50 kOe at different temperatures from 5 to 300 K. Zero-field-cooled (ZFC) and field-cooled (FC) magnetization was measured in the temperature region of 1.8–300 K, using applied fields of 0.1–20 kOe.

3. Results and discussion

Two samples were selected, $Fe_{2.85}Gd_{0.15}O_4$ and $Fe_{2.85}Tm_{0.15}O_4$ (labeled S1 and S2, respectively), in order to refine their structural and microstructural parameters using the Fullprof program [11], which allows refining the lattice parameters, atomic coordinates, site-occupancies, thermal parameters, and microstructural parameters simultaneously.

Both S1 and S2 samples could be refined using space group $Fd\bar{3}m$ with spinel type structure having Fe and Me (Me-Gd, Tm) atoms in the special Wyckoff positions 8a and 16d and O in the 32e. Starting model for the determination of the cation distribution was based on site preferences for cation sites in a spinel structure. Since iron ions can occupy both 8a and 16d sites, it was assumed for Gd^{3+} and Tm^{3+} ions were octahedrally coordinated. A deviation from stoichiometry was allowed during refinement of occupation numbers.

X-ray patterns were refined allowing the presence of secondary hematite α-Fe_2O_3 and a bcc iron belonging to hardened-steel balls in addition to the spinel phase. The best results were obtained using two-phase model: spinel + hematite. From the Rietveld's refinement procedure, an amount of about 2.1(1) % and 2.4(2) % of the α-Fe_2O_3 was obtained in S1 and S2 sample, respectively. Refinements continued till convergence was reached with a value of the agreement factor, χ^2 (χ^2—goodness of fit) close to 1 (1.23 and 1.19 for S1 and S2), which is the measure of how well the fitted model accounts for the data. Refined crystal structure parameters are given in Table 1.

The cation distribution in 8a (A) and 16d (B) crystallographic sites for spinels $Fe_{2.85}Gd_{0.15}O_4$ and $Fe_{2.85}Tm_{0.15}O_4$ was investigated through the refinement of the occupation numbers (N). As it can see from Table 1, Gd^{3+} and Tm^{3+} ions occupy only octahedral sites. These results were used as a basis for our interpretation of the magnetic properties. Finally, the crystallite size and strain and their anisotropy in samples were determined by refinements of the TCH-pV parameters and cubic harmonic function methods (incorporated in the Fullprof computer program). As it can be seen from Table 1, the average mixing strain value of $Fe_{2.85}Tm_{0.15}O_4$ is higher than the average mixing strain value of $Fe_{2.85}Gd_{0.15}O_4$. Taking in consideration earlier results on Fe_3O_4, $Fe_{2.85}Y_{0.15}O_4$ and $Fe_{2.55}In_{0.45}O_4$ [1], the average apparent strain increase in the following order: $Fe_{2.85}Tm_{0.15}O_4 < Fe_3O_4 < Fe_{2.85}Gd_{0.15}O_4 < Fe_{2.85}Y_{0.15}O_4 < Fe_{2.55}In_{0.45}O_4$. This fact could be explained by the influence of value of ionic radii of iron substituent and quantity of substituent (Gd^{3+}, Tm^{3+} and Y^{3+} ≈5% and In^{3+} ≈15%). Average apparent crystallite size dimensions increase in following order: $Fe_{2.85}Y_{0.15}O_4 < Fe_{2.85}Gd_{0.15}O_4 < Fe_{2.85}Tm_{0.15}O_4 < Fe_3O_4 < Fe_{2.55}In_{0.45}O_4$ what can be due to difference in cation radii of rare earth. It should bear in mind that all specimens were treated mechanochemicaly under the same conditions. The standard deviations appearing in the global average apparent size and strain (Table 1) is calculated using the different lattice direction. It is a measure of degree of anisotropy, not the estimated error.

The size anisotropy is small for $Fe_{2.85}Gd_{0.15}O_4$ and $Fe_{2.85}Tm_{0.15}O_4$ (see Table 1 and Figs. 1a and 2a). The strain anisotropy is high (see Table 1 and Figs. 1b and 2b) for both investigated samples, indicating nonuniform distribution of defects in the presence of Gd and Tm in the crystal structure. The strain anisotropy is more pronounced for $Fe_{2.85}Tm_{0.15}O_4$ then for $Fe_{2.85}Gd_{0.15}O_4$ and could be explained by the lower mixibility

Table 1
Crystal data and corresponding agreement factors for investigated specimens

Crystal system: face centered cubic	Space group: $Fd\bar{3}m$ (227)	
Composition	$Fe_{2.85}Gd_{0.15}O_4$	$Fe_{2.85}Tm_{0.15}O_4$
A		
Lattice parameter a (Å)	8.4118(4)	8.4076(3)
Cation–anion distance d (Å)		
$d(M_{8a}\text{-}O)$	1.8694(1) × 4	1.8561(1) × 4
$d(M_{16d}\text{-}O)$	2.0755(1) × 6	2.0814(1) × 6
Temperature factors U_{eq} (Å^2)		
U_{8a}	0.0120(5)	0.0140(4)
U_{16d}	0.0095(3)	0.0087(4)
U_{32e}	0.0129(12)	0.0129(12)
Occupation parameters N		
$N(Fe)_{8a}$	0.250(1)	0.250(1)
$N(Fe)_{16d}$	0.462(3)	0.464(4)
$N(Tm)_{16d}$		0.036(4)
$N(Gd)_{16d}$	0.038(3)	
$N(O)_{32e}$	1.000(1)	1.000(1)
Agreement factors		
cR_p (%)	11.9	9.11
cR_{wp} (%)	15.7	11.8
R_B (%)	7.16	5.14
χ^2	1.23	1.19
D	1.68	1.75
Average apparent size (Å)	72(8)	85(15)
Average app. strain (×10^4)	31(12)	41(15)

Please cite this article in press as: Z. Cvejic, et al., J. Alloys Compd. (2008), doi:10.1016/j.jallcom.2008.05.026

between Fe and Tm then between Fe and Gd in a spinel structure [12,13].

We used transmission electron microscopy image to investigate particle size and morphology. Fig. 3 shows the TEM images for $Fe_{2.85}Tm_{0.15}O_4$ sample. The analysis revealed that the particles have a particle size distribution with mean value of ~20 nm. This value is larger than the crystallite size obtained from Rietveld method (Table 1), suggesting that the particles are composed of several crystallites. Similar conclusions apply for $Fe_{2.85}Y_{0.15}O_4$, having particle size of c.a. 17 nm [1].

In order to analyze magnetic behavior of the samples $Fe_{2.85}RE_{0.15}O_4$ (RE = Y, Gd, Dy, Ho, Tm and Yb) as well as $Fe_{2.55}In_{0.45}O_4$, we measured magnetization versus temperature $M(T)$, and magnetization versus field, $M(H)$, at 2 K.

Experimental results, $M(T)$, are shown on Fig. 4. It can be seen that the zero-field-cooled magnetization curves display a broad maximum centered at T_{max}, as expected for superparamagnetic (SPM) unblocking process in single/domain particles. Having a size distribution, T_{max} is related to the average blocking temperature T_B of the particles, which become superparamagnetic at $T > T_{max}$. T_B values for applied field of 100 Oe were found to be about 200 K. The Field-cooled magnetization curves do not merge the ZFC data within our experimental temperature range, reflecting the distribution of blocking temperatures related to size dispersion of the particles. In agreement with the known dependence of T_B with applied field, it is observed that T_{max} decreases for larger applied fields (inset of Fig. 4). Concurrently, the ZFC and FC magnetization branches separate at a much lower temperature T_{ir} when the applied field is 20 kOe ($Fe_{2.55}In_{0.45}O_4$). It is worth noting that these T_B values were obtained in concentrate powders, so they do not reflect the blocking temperatures of isolated (non/interacting) particles. Moreover, many different factors can influence the T_B values in a nanoparticle system, including magnetic anisotropy, or interparticle interactions.

For $H = 100$ Oe, field cooled–zero-field-cooled magnetization difference, $M(FC) - M(ZFC)$, is large (Fig. 4). However, this difference decreases with increase of the magnetic field and becomes very small for applied fields of 20 kOe ($Fe_{2.55}In_{0.45}O_4$). It is known that strong magnetic irreversibility disappears when the anisotropy field of the particles is surpassed by an applied field and the particles are supposed to be saturated. It takes place in the fields of few kOe [14]. However, strong magnetization irreversibility was found

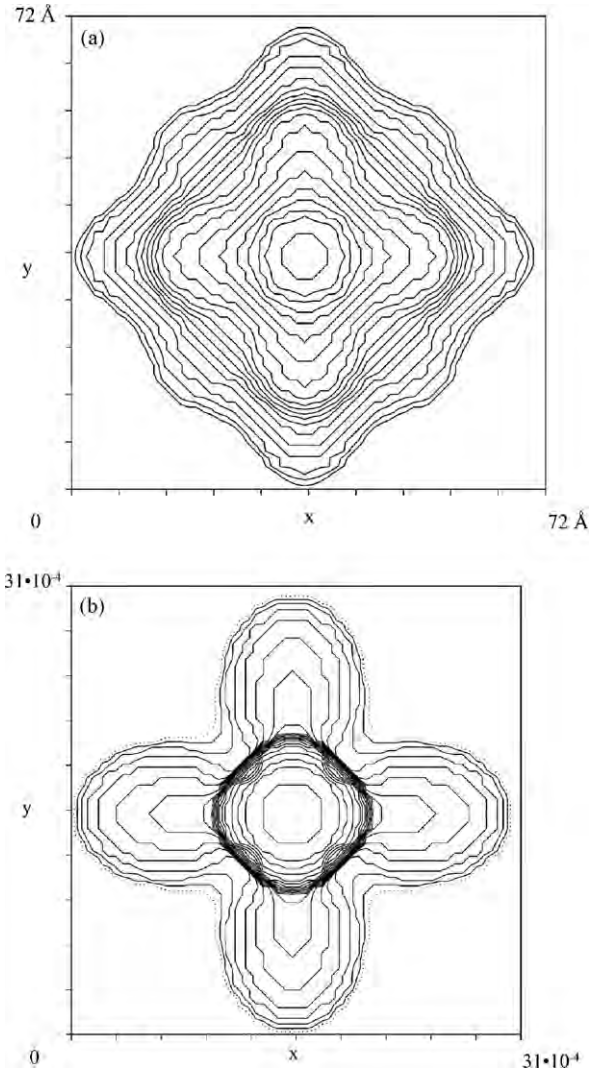

Fig. 1. (a) Projections of the three-dimensional body that represents "apparent ctystallite size" in the (0 0 1) crystallographic plane for $Fe_{2.85}Gd_{0.15}O_4$ and (b) projections of the three-dimensional body that represents 'average max-strain'in the (0 0 1) crystallographic plane for $Fe_{2.85}Gd_{0.15}O_4$.

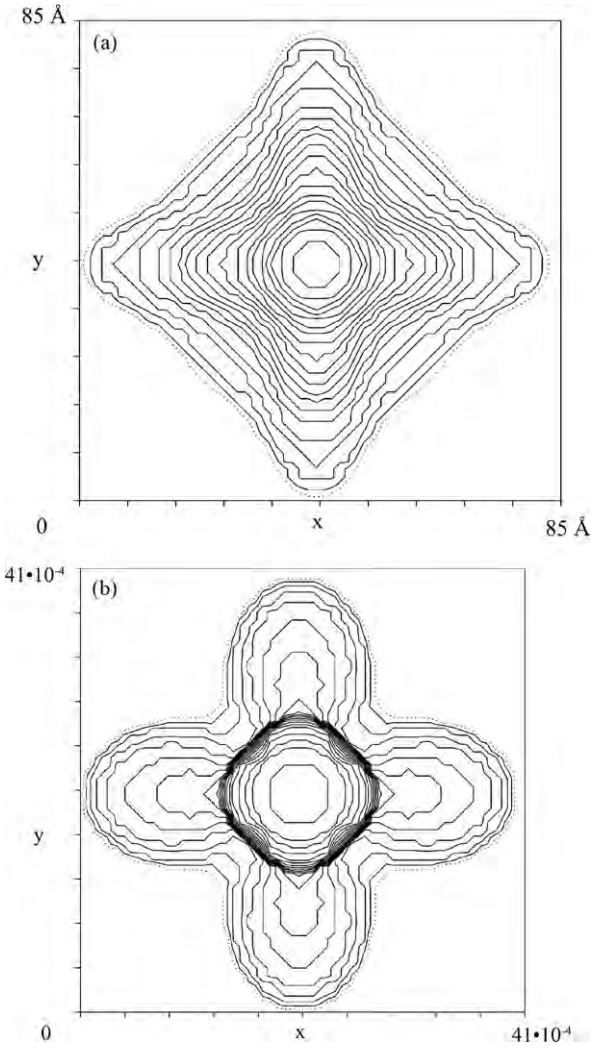

Fig. 2. (a) Projections of the three-dimensional body that represents "apparent ctystallite size" in the (0 0 1) crystallographic plane for $Fe_{2.85}Tm_{0.15}O_4$ and (b) projections of the three-dimensional body that represents 'average max-strain' in the (0 0 1) crystallographic plane for $Fe_{2.85}Tm_{0.15}O_4$.

Please cite this article in press as: Z. Cvejic, et al., J. Alloys Compd. (2008), doi:10.1016/j.jallcom.2008.05.026

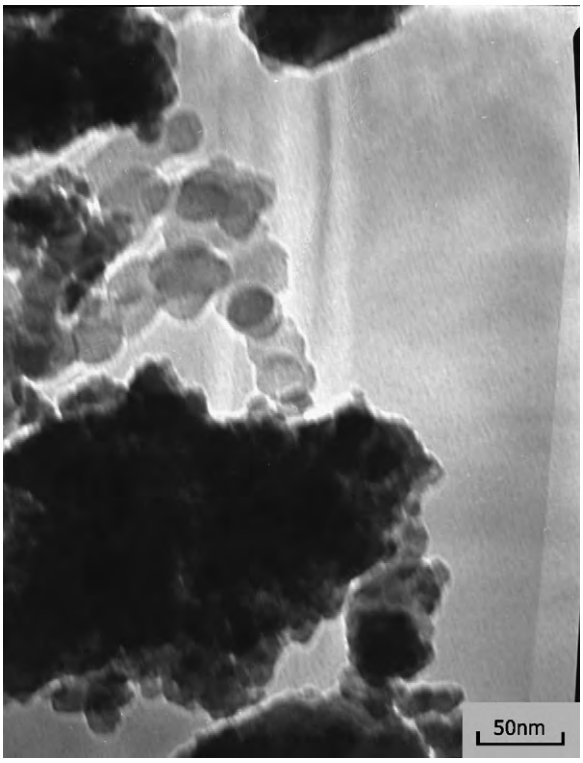

Fig. 3. TEM micrograph of $Fe_{2.85}Tm_{0.15}O_4$.

in some nanosize ferrites even at fields of 70 kOe in Ni-ferrite [14], 80 kOe in Zn-ferrite [15] and 55 kOe in γ-Fe_2O_3 [16]. The high field magnetic irreversibility found in the $Fe_{2.55}In_{0.45}O_4$ is consequence of high anisotropy.

Magnetization versus field, $M(H)$, of $Fe_{2.85}RE_{0.15}O_4$ (RE = Y, Gd, Dy, Ho, Tm and Yb) and $Fe_{2.55}In_{0.45}O_4$ was measured at $T = 2$ K. $M(H)$ curves are shown at Figs. 5 and 6. Up to 50 kOe, magnetization does not saturate, which can be attributed to spin disorder induced by the milling process. Saturation magnetization M_S was obtained by extrapolating the $M(1/H)$ dependence on $1/H = 0$ value. The found M_S, remanent magnetization, M_R and coercivities, H_C values are reported in Table 2. The largest M_S was found in

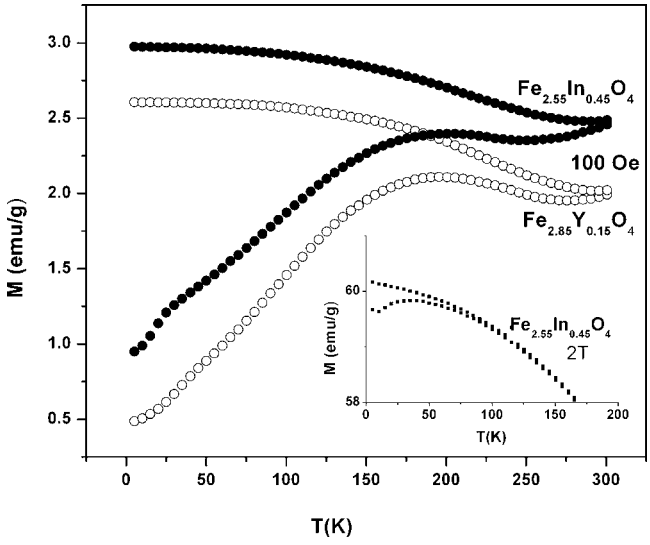

Fig. 4. Magnetization versus temperature for $Fe_{2.55}In_{0.45}O_4$ and $Fe_{2.85}Y_{0.15}O_4$.

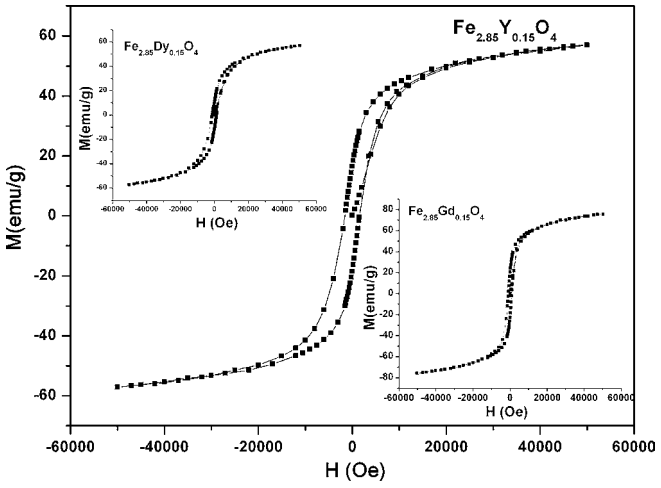

Fig. 5. Magnetization versus field of $Fe_{2.85}RE_{0.15}O_4$ (RE = Tm, Ho) and $Fe_{2.55}In_{0.45}O_4$ at 2 K.

Gd-substituted magnetite, while the smallest was observed in Y-substitute magnetite, where the largest coercivity was observed. Remanence M_R was found to have values from 11 to 20.5 emu/g. Inspection of reported values in Table 2 does not show any regularity with increasing ionic radii, and more careful analysis is required of obtained magnetic parameters. Consequently, the following effects on the magnetization value were considered: (i) magnetic anisotropy, (ii) particle size effect, (iii) cation distribution, (iv) chemical composition and (v) the presence of parasite phases.

The common types of anisotropies in nanosize materials are magnetocrystalline, shape and strain induced anisotropy. The magnetocrystalline anisotropy depends on the spin-orbit (L–S) coupling and energetically favors alignment of the magnetization along a specific crystallographic direction (easy axis of the magnetization). The strength of the coupling at RE^{3+} sites depends on type of cation, and can be very different, dramatically changing magnetic parameters [17].

Particle morphology investigated by TEM revealed that the particles were nearly spherical in shape. As found above and in our earlier paper [1], the X-ray line broadening anisotropy due to crystallite size effect is significant in Y- and In-substituted magnetite, while strain anisotropy is small. Opposite case was found in the present work for magnetite with Tm and Gd. From these results it

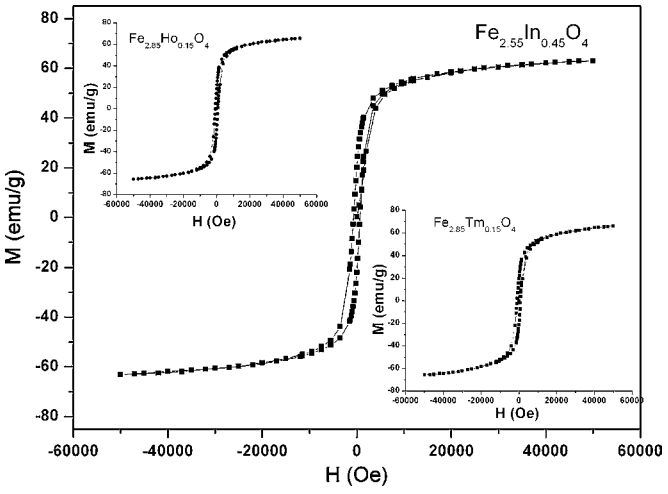

Fig. 6. Magnetization versus field of $Fe_{2.85}RE_{0.15}O_4$ (RE = Y, Gd, Dy) at 2 K.

Table 2
Magnetic parameters of RE substituted magnetite

Sample	2 K		
	M_S (emu/g)	H_C (Oe)	M_R (emu/g)
$Fe_{2.55}In_{0.45}O_4$	63	700	20.5
$Fe_{2.85}Y_{0.15}O_4$	57	1550	16.4
$Fe_{2.85}Gd_{0.15}O_4$	77	900	20
$Fe_{2.85}Dy_{0.15}O_4$	58	1213	11
$Fe_{2.85}Ho_{0.15}O_4$	68	800	19
$Fe_{2.85}Tm_{0.15}O_4$	66	880	19
$Fe_{2.85}Yb_{0.15}O_4$	60	1100	17

can be concluded that the shape and strain anisotropy influence magnetic behavior of studied samples.

Size effect in ferromagnetic nanoparticles is often a cause of the magnetization reduction in comparison with the values obtained for the bulk counterparts. Namely, the decrease in particle size increases the surface to volume ratio, forming the surface uncompensated magnetic moments (shell) which is responsible for significant reduction of net magnetization. Šepelak et al. found enhancement of magnetization in nanosized Mg ferrite synthesized by high energy ball milling [18,19]. It was shown large influence of surface shell (with the thickness of 0.9 nm) on magnetization, larger than one of particle core. Although here studied samples were prepared under the same conditions, the value of crystallite size varies from 6.8 nm in $Fe_{2.85}Y_{0.15}O_4$ to 18.4 nm in $Fe_{2.55}In_{0.45}O_4$ [1].

The intensity of exchange interactions (A–B, A–A and B–B) is determined by cation occupancies, so that the net magnetization depends on cation distribution. The change of cation distribution in nanoparticle did not lead to enhancement of the saturation magnetization of its bulk counterpart [20]. Equal quantity of Fe^{3+} ions at B sites is substituted by non-magnetic Y^{3+} or magnetic RE^{3+} (RE = Gd, Dy, Ho, Tm and Yb). Non-magnetic ion substitution influences by lowering of strength of superexchange interactions (A–B and B–B). Effective magnetic moments of Gd^{3+}, Dy^{3+}, Ho^{3+}, Tm^{3+} and Yb^{3+} are higher than Fe^{3+}, so the superexchange interactions increase with substitution. Consequently, magnetization in the magnetic ions substituted magnetite is somewhat higher, Table 2. The lowest M_S was observed in $Fe_{2.85}Y_{0.15}O_4$ (the highest in $Fe_{2.85}Gd_{0.15}O_4$). A random cation distribution was obtained in $Fe_{2.55}In_{0.45}O_4$, with 33% of In^{3+} is on A sites [1]. Non-magnetic In^{3+} ions distribution influences all type of superexchange interactions, while In^{3+} was in the higher percentage incorporated in magnetite.

Considering coercivity (Table 2), enhancement was observed for Y-substituted magnetite (while M_S is the lowest). The value is doubled in comparison with those of the In- and Ho-substituted magnetite. Similarly as it was discussed for M_S, crystalline anisotropy strongly influence to coercivity. Size/strain analysis has shown that strain induced anisotropy is significant. Strain induced anisotropy can additionally increase the H_C values due to hardening of the particle surface, which can be up to 10% of the total atoms for 15–20 nm particles.

4. Conclusion

High energy ball milling was used to prepare RE-substituted magnetite. The observed changes in M_S and H_C for $Fe_{2.85}RE_{0.15}O_4$ family is influenced by different factors, which were discussed, in order to emphasize importance of structure and microstrucural parameters that are dependent on preparation method. Thus, the obtained magnetic results on rare earth substituted magnetite can be useful for application, through manipulation with chemical composition and synthesis procedure. Additionally, partial cation substitution of iron by the rare earth elements stabilizes magnetite and preserves its structure from transition to hematite. This could be signification in different area of applications.

Acknowledgments

The Serbian Ministry of Science and Environmental Protection has financially supported this work. We thanks to Dr. N. Bibic for performing TEM images.

References

[1] Z. Cvejic, S. Rakic, A. Kremenovic, B. Antic, C. Jovalekic, Ph. Colomban, Sol. State Sci. 8 (2006) 908.
[2] E. Schmidbauer, R. Keller, J. Magn. Magn. Mat. 152 (1996) 99.
[3] M.H. Sousa, F.A. Tourinho, J. Depeyrot, G.J. Da Silva, M.C.F. Lara, J. Phys. Chem. B 105 (2001) 1169.
[4] Q.A. Pankhurst, J. Connolly, S.K. Jones, J. Dobson, J. Phys. D: Appl. Phys. 36 (2003) R167.
[5] G.F. Goya, V. Grazú, M.R. Ibarra, Curr. Nanosci. 4 (2008) 1.
[6] E.J.W. Verwey, Nature 144 (1939) 327.
[7] B. Antic, A. Kremenovic, A.S. Nikolic, M. Stoiljkovic, J. Phys. Chem. B 108 (2004) 12646.
[8] S.E. Jacobo, S. Duhalde, H.R. Bertorello, J. Magn. Magn. Mat. 272–276 (2004) 2253.
[9] R.V. Upadhyay, A. Gupta, C. Sudakar, K.V. Rao, K. Parekh, R. Desai, R.V. Mehta, J. Appl. Phys. 99 (2006), 08M906.
[10] A.K. Gupta, M. Gupta, Biomaterials 26 (2005) 3995.
[11] J.Rodriguez-Carvajal, FullProf.2k (Version 2.40-May 2003-LLB JRC) Computer program; http://www-llb.cea.fr/fullweb/fp2k/fp2k.htm.
[12] H.J. Van Hook, J. Am. Ceram. Soc. 45 (1962) 369.
[13] S.J. Schneider, R.S. Roth, J.L. Waring, J. Res. Natl. Bur. Stand., Sect. A 65 (4) (1961) 345.
[14] R.H. Kodama, A.E. Berkowitz, E.J. McNiff, S. Foner, Phys. Rev. Lett. 77 (1996) 394.
[15] G.F. Goya, H.R. Rechenberg, J. Magn. Magn. Mat. 203 (1999) 141.
[16] B. Martinez, X. Obradors, L. Balcells, A. Rouanet, C. Monty, Phys. Rev. Lett. 80 (1998) 181.
[17] Q. Song, Z.J. Zhang, J. Phys. Chem. B 110 (2006) 11205.
[18] V. Šepelak, I. Bergmann, D. Menzel, A. Feldhoff, P. Heitjans, F.J. Litterst, K.D. Becker, J. Magn. Magn. Mater. 316 (2007) E764.
[19] V. Šepelak, et al., Chem. Mat. 18 (2006) 3057.
[20] U. Luders, M. Bibes, J.-F. Bobo, M. Cantoni, R. Bertacco, J. Fontcuberta, Phys. Rev. B71 (2005) 134419.